

# LipidUNet-Machine Learning-Based Method of Characterization and Quantification of Lipid Deposits Using iPSC-Derived Retinal Pigment Epithelium

Zander Esh<sup>\*1</sup>, Sharanya Suresh<sup>\*1</sup>, Davide Ortolan<sup>1</sup>, Mitra Farnoodian<sup>1</sup>, Devika Bose<sup>1</sup>, Jiwon Ryu<sup>1</sup>, Andrei Volkov<sup>1</sup>, Kapil Bharti<sup>1</sup>, Ruchi Sharma<sup>1</sup>

<sup>1</sup>Ocular and Stem Cell Translational Research Section, National Eye Institute, National Institutes of Health (NIH)

\*These authors contributed equally

## Corresponding Authors

**Kapil Bharti**

kapil.bharti@nih.gov

**Ruchi Sharma**

fnu.ruchi2@nih.gov

## Citation

Esh, Z., Suresh, S., Ortolan, D., Farnoodian, M., Bose, D., Ryu, J., Volkov, A., Bharti, K., Sharma, R. LipidUNet-Machine Learning-Based Method of Characterization and Quantification of Lipid Deposits Using iPSC-Derived Retinal Pigment Epithelium. *J. Vis. Exp.* (197), e65503, doi:10.3791/65503 (2023).

## Date Published

July 28, 2023

## DOI

10.3791/65503

## URL

jove.com/video/65503

## Abstract

The retinal pigment epithelium (RPE) is a monolayer of hexagonal cells located at the back of the eye. It provides nourishment and support to photoreceptors and choroidal capillaries, performs phagocytosis of photoreceptor outer segments (POS), and secretes cytokines in a polarized manner for maintaining the homeostasis of the outer retina. Dysfunctional RPE, caused by mutations, aging, and environmental factors, results in the degeneration of other retinal layers and causes vision loss. A hallmark phenotypic feature of degenerating RPE is intra and sub-cellular lipid-rich deposits. These deposits are a common phenotype across different retinal degenerative diseases. To reproduce the lipid deposit phenotype of monogenic retinal degenerations *in vitro*, induced pluripotent stem cell-derived RPE (iRPE) was generated from patients' fibroblasts. Cell lines generated from patients with Stargardt and Late-onset retinal degeneration (L-ORD) disease were fed with POS for 7 days to replicate RPE physiological function, which caused POS phagocytosis-induced pathology in these diseases. To generate a model for age-related macular degeneration (AMD), a polygenic disease associated with alternate complement activation, iRPE was challenged with alternate complement anaphylatoxins. The intra and sub-cellular lipid deposits were characterized using Nile Red, boron-dipyrromethene (BODIPY), and apolipoprotein E (APOE). To quantify the density of lipid deposits, a machine learning-based software, LipidUNet, was developed. The software was trained on maximum-intensity projection images of iRPE on culture surfaces. In the future, it will be trained to analyze three-dimensional (3D) images and quantify the volume of lipid droplets. The LipidUNet software will be a valuable resource for discovering drugs that decrease lipid accumulation in disease models.

## Introduction

The retinal pigment epithelium (RPE) is a monolayer of cells located in the back of the eye adjacent to retinal photoreceptors. RPE plays a vital role in maintaining proper vision by providing metabolic and structural support to the photoreceptors. Healthy RPE cells are characterized by a distinct hexagonal morphology. They are connected by tight junctions, which allow the RPE to act as a barrier between the choriocapillaris located on its basal side and photoreceptors located apically. To maintain the retinal ecosystem, RPE shuttles key metabolites, e.g., glucose, to photoreceptors in a way that minimizes glucose consumption in the RPE<sup>1</sup>. Due to this limitation, RPE depends on other metabolites to maintain their metabolic needs, including fatty acids, which RPE converts to ketones through  $\beta$ -oxidation<sup>2</sup>. Given the propensity of RPE to utilize fatty acids, which are likely recycled from photoreceptor outer segment (POS) digestion, as an energy source, detrimental changes to the lipid processing pathways in RPE often lead to, or are implicated in, both monogenic and polygenic degenerative retinal diseases<sup>3</sup>.

Age-related macular degeneration (AMD), a polygenic degenerative eye disease that causes RPE degeneration, has also been linked to aberrant autophagy and lipid metabolism in the RPE monolayer. The failure of a dysfunctional RPE monolayer to process POS and perform other critical functions leads to extracellular (sub-RPE) deposits called basal linear deposits (BLinD) located between the RPE and Bruch's membrane - a hallmark of AMD pathologies. Major components of BLinD include lipoproteins, the most abundant of which is apolipoprotein E (APOE)<sup>4</sup>.

Accumulation of thin layers of BLinD can lead to soft drusen, which is recognized as a clinical symptom of AMD<sup>5,6</sup>.

Several groups have shown that stem cell-derived *in vitro* disease models that cause RPE dysfunction feature sub-RPE lipid accumulation<sup>7,8,9</sup>. Hallam et al. (2017) generated induced pluripotent stem cell-derived RPE (iRPE) from patients with a high risk for AMD due to a polymorphism of the *CFH* gene. The iRPE showed drusen accumulation, as marked by APOE, and the high-risk RPE accumulated larger deposits than iRPE generated from low-risk patients<sup>10</sup>.

To create an *in vitro* model that recapitulates cellular hallmarks of AMD, such as lipid droplets and drusen deposition, iRPE lines generated from patient blood samples were established using a previously published developmentally guided protocol<sup>11</sup>. The iRPE were subjected to complement-competent human serum (CC-HS), a solution containing anaphylatoxins that mimic one possible cause of AMD: increased alternate complement signaling<sup>8</sup>. The resulting cellular and sub-cellular deposition of lipid deposits was measured using commonly used lipid and lipoprotein markers, APOE, Nile Red, and BODIPY. Through these markers, it was shown that activated complement signaling via CC-HS exacerbated lipid accumulation in iRPE cells<sup>8</sup>.

To develop a disease model for a monogenic retinal degenerative disease, iRPE lines were developed from patients with Stargardt disease, a disease caused by mutations to the *ABCA4* gene in RPE. It has previously been shown that when *ABCA4* is knocked out, A2E lipofuscin, an intracellular deposit known to contain high levels of phospholipids and light-dependent lipid peroxidation products, accumulates inside the RPE<sup>12</sup>. *ABCA4* knockout

lines were developed alongside the patient lines, and both were subjected to POS feeding. The Stargardt iRPE demonstrated POS phagocytosis-induced pathology, exhibiting increased lipid accumulation quantified by BODIPY staining. RPE derived from *ABCA4* KO iPSCs were subjected to CC-HS treatment; quantification of the BODIPY signal showed a defect in lipid handling in the Stargardt disease model as well<sup>9</sup>.

Given the prevalence of these diseases and the need for effective therapeutics, along with the relevant disease models described above, there is a need to establish

robust methods for quantifying the efficacy of potential treatments. To quantify lipid deposits in a way that is objective, automated, and standardized, a machine-learning-based software, LipidUNet, was created so that, when paired with mask analysis tools, lipid deposition can quickly and effectively be identified using the common markers Nile Red, BODIPY, and APOE. The summary statistics obtained using this analysis pipeline can then be analyzed and displayed graphically, allowing for easy comparison of treatment conditions. The schematic of the protocol is shown in **Figure 1**.

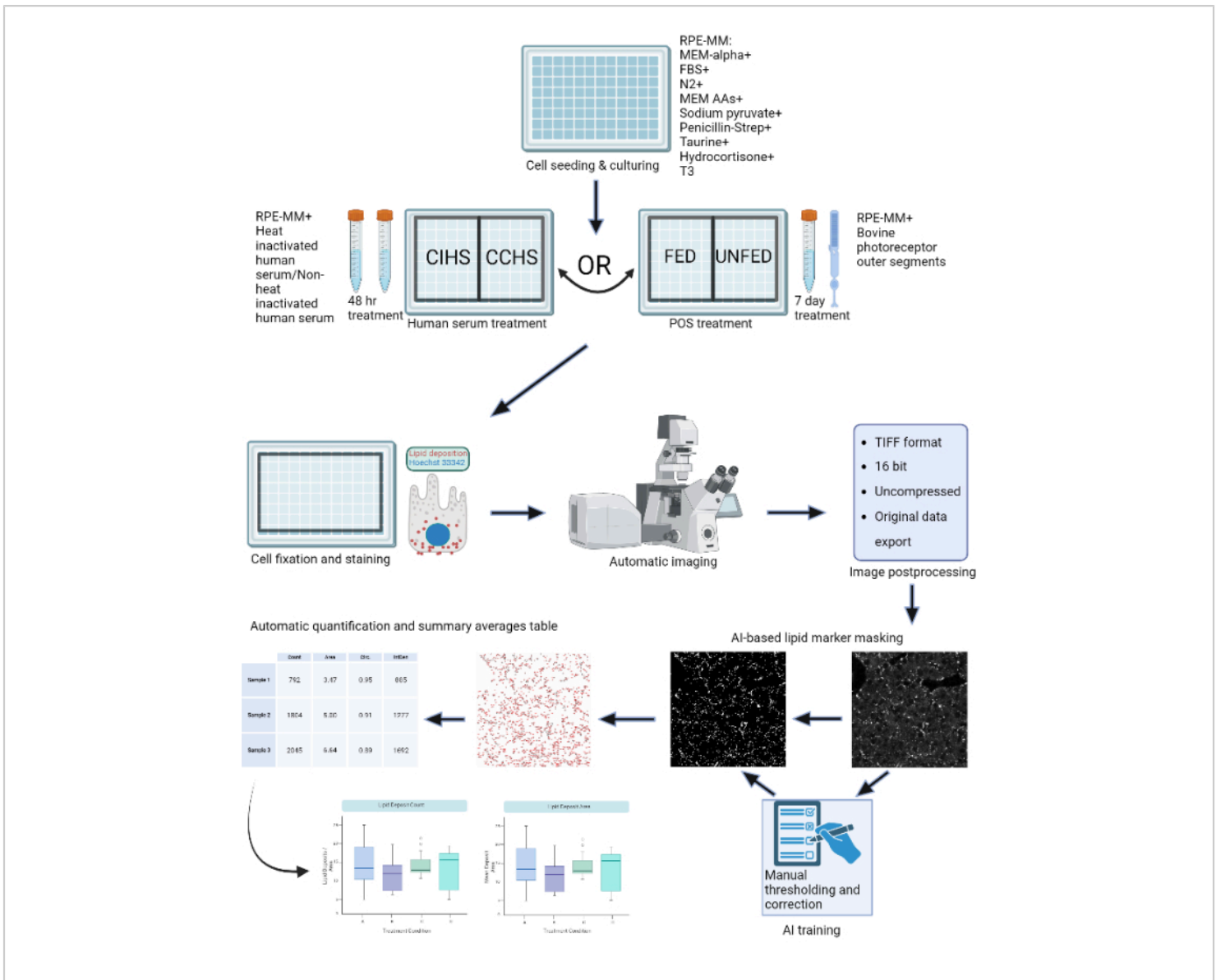


**Figure 1: Schematic of the protocol:** RPE cells are grown on a 96-well plate and challenged with active human serum or purified bovine outer segments to model different types of retinal degenerations *in vitro*. RPE cells are fixed and stained for lipoprotein deposits with Nile Red, BODIPY, and APOE. A confocal microscope is used to acquire Z-stacks of fluorescently-labeled lipid particles, which are subsequently processed into 2D maximum intensity projections. A machine-learning algorithm was trained to recognize and correctly segment lipoprotein particles. Summary tables containing particle count and various shape metrics are generated and can be used for subsequent plotting and statistical analysis. [Please click here to view a larger version of this figure.](#)

## Protocol

All protocol steps adhere to the guidelines set forth by the NIH's human research ethics committee. Stem cell work and patient sample collection were approved by the Combined NeuroScience Institutional Review Board (CNS IRB) under the Office of Human Research Protection (OHRP), NIH, as per 45 CFR 46 guidelines of the U.S. Government. Patient samples were collected using CNS

IRB-approved consent form in accordance with the criteria set by the Declaration of Helsinki under the protocol number NCT01432847 (<https://clinicaltrials.gov/ct2/show/NCT01432847?cond=NCT01432847&draw=2&rank=1>).

### 1. iRPE generation

1. Generate iRPE from patient blood-derived iPSC following the published protocol by Sharma et al., 2022<sup>11</sup> (Figure 2 and Figure 3).

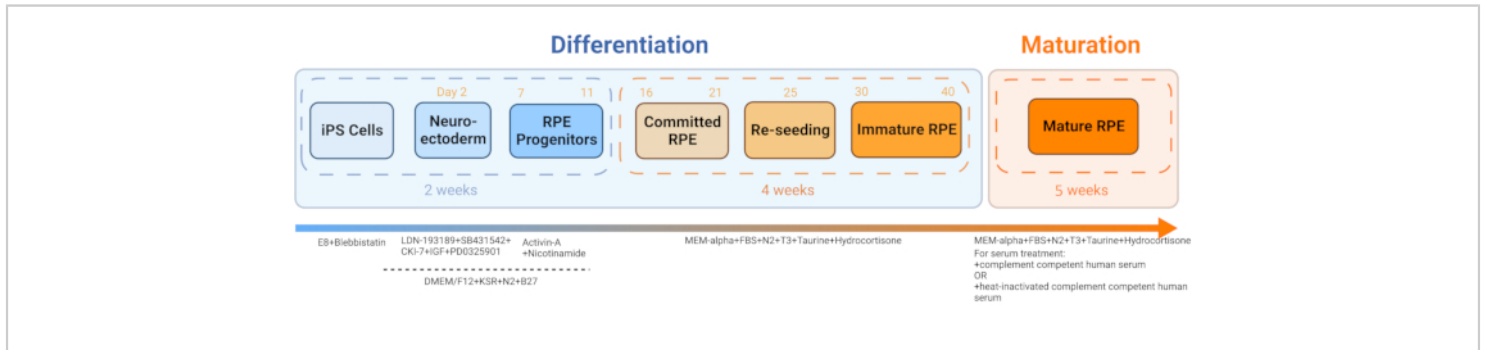


**Figure 2: Schematic of iRPE differentiation and maturation.** To generate iRPE, an established differentiation protocol was followed, and the cells were allowed to mature for 5 weeks. The resulting cell culture acts as an *in vitro* model that can be manipulated with various treatments to mimic RPE dysfunction in diseases like AMD and Stargardt disease. [Please click here to view a larger version of this figure.](#)

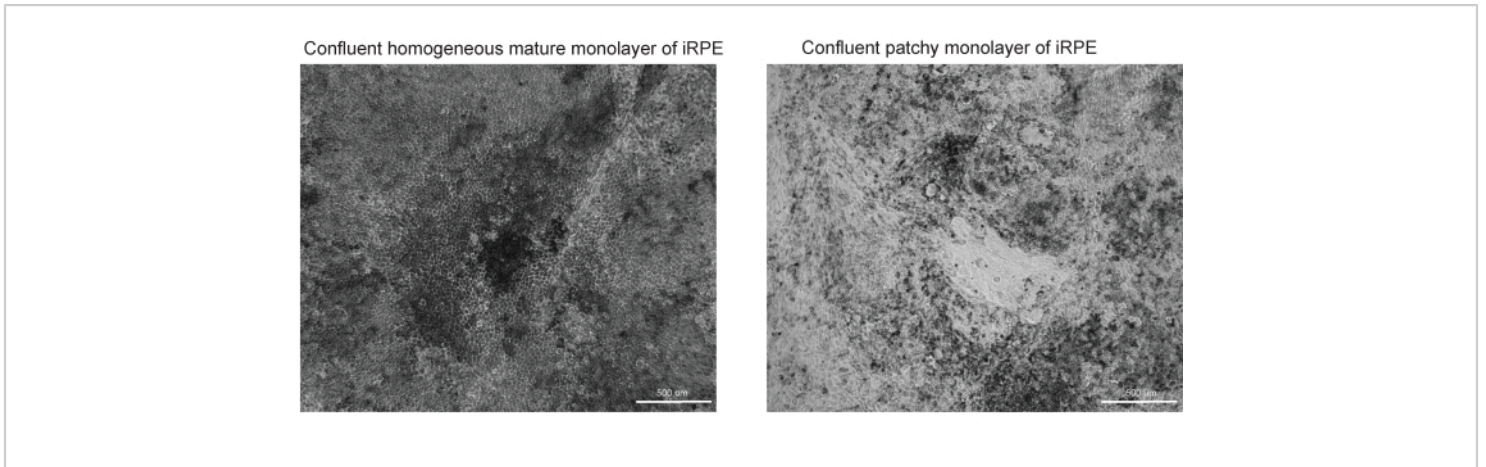


**Figure 3: Representative images of successful and unsuccessful RPE differentiation and maturation.** Two brightfield images at 10x magnification of TJP1 RPE are shown at Day 42 of the iRPE protocol. **(A)** Successful differentiation and maturation will show confluent RPE with pigmentation and polygonal morphology. **(B)** Unsuccessful differentiation and maturation will show clusters of dying cells, as shown here. [Please click here to view a larger version of this figure.](#)

## 2. RPE maintenance media (RPE-MM) preparation

1. Thaw the N2 supplement at 4 °C overnight. Thaw all other reagents at room temperature (RT).
2. Under sterile conditions, add the reagents listed in **Table 1** at the listed dilution factors, as per the protocol established by Sharma et al., 2022<sup>11</sup>.
3. Mix the media well and filter it using a 0.22 μm filtration unit.

**NOTE:** Media is suitable for use within 2 weeks if stored at 4 °C.

## 3. 96-well plate seeding

1. Thaw an aliquot of vitronectin at RT for 3-5 min or until the ice is completely melted.
2. Dilute the vitronectin with 1x Dulbecco's phosphate-buffered saline (DPBS) to obtain the desired working solution using a 1:200 dilution (vitronectin: DPBS). For a

96-well plate, coat each well with 200 μL of the working solution.

3. Combine thawed ROCK inhibitor (Y-27632 dihydrochloride) with the RPE-MM at a 1:1000 dilution to achieve a final concentration of 10 μM. This is the plating media for RPE cells.
4. Thaw the iRPE vial using an automated cell thawing system and transfer the iRPE cell suspension to a 50 mL tube.
5. Dilute the cell suspension with the plating media at a 1:10 dilution. Centrifuge the tube at 400 x g for 5 min.
6. Carefully aspirate the supernatant and resuspend the cells in 10 mL of the plating media.
7. Mix 400 μL of the plating media with 100 μL of the resuspended cell solution for cell counting. Use this aliquot to determine the viable cell concentration of the cell suspension using a cell viability counter.

8. Dilute the cell suspension with the plating media to a final concentration of 60,000 cells/mL.
  9. Completely aspirate the vitronectin coating solution from the 96-well plate and dispense 200  $\mu$ L of the cell suspension into each well. There will be roughly 12,000 cells/well or  $\sim$ 200 cells/ $\text{mm}^2$ .
  10. Incubate the seeded cell plates for 48 h at 37  $^{\circ}$ C and 5%  $\text{CO}_2$ . After 48 h, change the media to RPE-MM without ROCK inhibitor supplement. Change the media every 2-3 days during the 5-week maturation period.
4. Wash the cells with 1x DPBS and fix them with 4% paraformaldehyde for 20 min at RT. Wash once more with 1x DPBS and store the samples at 4  $^{\circ}$ C, immersed in 200  $\mu$ L of DPBS.
  5. OPTIONAL: If desired, lyse the cells from the plate to show only sub-RPE lipid deposition.
    1. To lyse the cells and leave only lipid deposits, remove the media and add 200  $\mu$ L of deionized water to each well.
    2. Incubate for 10-15 min, pipette up and down until cells are removed. Wash once more with 200  $\mu$ L of deionized water and immediately fix the cells with 4% paraformaldehyde.
    3. Confirm the cell removal efficacy with nuclear staining using Hoechst. Add Hoechst at 1:2000 dilution to a 1x DPBS solution containing 1% bovine serum albumin (BSA), 0.5% Tween 20, and 0.5% Triton-X 100. Incubate at RT for 1 h in the dark. Subsequently, wash with 1x DPBS.

#### 4. *In vitro* disease models

1. Complement competent human serum (CC-HS) treatment
  1. Thaw human complement competent serum at 4 $^{\circ}$ C overnight.
  2. Prepare CC-HS and complement incompetent human serum (CI-HS) media.
    1. To prepare 5% CC-HS media, mix the thawed complement competent human serum with RPE-MM at a 1:20 dilution. Filter the solution through a 0.22  $\mu$ m media filter before use.
    2. To prepare 5% complement incompetent human serum (CI-HS) media, first heat inactivate the CC-HS in a 57  $^{\circ}$ C water bath for 30 min and then mix with the culture media at a 1:20 dilution. Filter the solution through a 0.22  $\mu$ m media filter before use.
  3. Serum treat the cells with 200  $\mu$ L of either 5% CC-HS or 5% CI-HS media for a total incubation time of 48 h, refreshing the media after 24 h.
2. Photoreceptor outer segment (POS) treatment on iRPE
  1. POS preparation
    1. Remove the POS pellet tube from -80  $^{\circ}$ C storage and thaw overnight at 4  $^{\circ}$ C in a covered ice bucket.
    2. Prepare POS wash buffer by mixing 10 g of sucrose in 40 mL of double-deionized  $\text{H}_2\text{O}$  (dd $\text{H}_2\text{O}$ ).
    3. Heat mixture at 40-50  $^{\circ}$ C while gently stirring for 15 min. Add 840 mg of sodium bicarbonate to the mixture and stir while heating for 10 min.

4. Adjust the total volume of the POS wash buffer to 100 mL with ddH<sub>2</sub>O and adjust the pH of the solution to 8.3 with 1 N HCl or 1 N NaOH, as needed. Filter the wash solution using a 0.22 µm filter.

**NOTE:** The protocol can be paused here; the POS wash buffer can be stored at 4 °C overnight.

5. Once thawed, suspend the pellet in 15 mL of POS wash buffer. Be gentle during pellet suspensions to ensure POS integrity. Centrifuge the POS suspension at 600 x g at 4 °C for 20 min and then aspirate the supernatant.
6. Resuspend the POS pellet in 10 mL of the POS wash buffer.
7. Remove a 100 µL aliquot of the POS + POS wash buffer (POS solution) and dilute in 400 µL of 1x DPBS. Spread 50 µL of the diluted POS solution on a blood agar plate and an agarose plate to check for bacterial and fungal contaminants. Prepare positive controls for each and incubate all plates for 48 h at 37 °C.
8. Perform a qPCR assay by adding 1 µL of POS solution to the detection well to test for mycoplasma. To amplify DNA fragments, perform 40 cycles of denaturation (95°C, 15 s), and annealing and elongation (60°C, 1 min). The forward and reverse primers for detecting mycoplasma in the POS sample are as follows:  
Forward primer: GGA TTA GAT ACC CTG GTA GTC CAC G  
Reverse primer: CGT CAA TTC CTT TAA GTT TCA CTC TTG GC

9. Measure POS concentration using a cell analyzer and aliquot according to need. For one well of 96 well plates with RPE cells, 3 x 10<sup>6</sup> POS is sufficient. The desired ratio is 10 POS/RPE cell. Store the aliquots at 80 °C for future use.

## 2. Addition of POS to cells

1. Thaw vials of POS in an ice bath.
2. Mix the calculated amount of prepared POS with RPE-MM and treat the cells with POS once daily for 7 days.

**NOTE:** Prepare POS solution fresh daily.

3. Wash the cells with 1x DPBS and then fix them with 4% paraformaldehyde for 20 min at RT. Wash with DPBS once more and store samples at 4 °C, immersed in 200 µL of DPBS.

## 5. Staining for sub-RPE deposits

### 1. Nile red staining protocol

1. After PFA fixation, wash the samples 3 times with 1x DPBS.

**NOTE:** If not used immediately, the protocol can be paused here, but samples must be stored in a 1x DPBS + 0.02% sodium azide solution at 4 °C.

2. To prepare the Nile Red stock solution, dissolve Nile Red powder in acetone at 3 mg/mL concentration. Incubate for 15 min at RT with periodic mixing. Filter the solutions with a 0.22 µm filter once or twice depending on the level of precipitate remaining in the solution.

**NOTE:** Protect the stock solution from light.

3. To prepare the working solution, dilute the stock solution at a ratio of 1:500 in 1x DPBS. Add 200  $\mu$ L of the working solution to the sample for 30 min at RT on a shaker and protect it from light.
4. Wash 3 times with 1x PBS and store the samples at 4  $^{\circ}$ C, immersed in 200  $\mu$ L of DPBS.

**NOTE:** If conducting an experiment on transwells instead of a 96-well plate, samples can be mounted on a slide with mounting media, covered with a glass coverslip, and sealed with transparent nail polish. Care should be taken to mount the sample with the cells facing up.

## 2. BODIPY staining protocol

1. For stock solution, dissolve BODIPY in anhydrous dimethyl sulfoxide (DMSO) to attain a stock concentration of 3.8 mM.
2. For PFA fixed samples, dilute BODIPY stock at 1:300 in 1x DPBS. Add 200  $\mu$ L to cells and incubate overnight on a rocker at RT.
3. Wash 3 times with 1x DPBS and store the samples at 4  $^{\circ}$ C, immersed in 200  $\mu$ L of DPBS.

**NOTE:** If conducting an experiment on transwells instead of a 96-well plate, samples can be mounted on a slide with mounting media, covered with a glass coverslip, and sealed with transparent nail polish. Care should be taken to mount the sample with the cells facing up.

## 3. APOE immunostaining protocol

1. Combine 1x DPBS with 1% bovine serum albumin (BSA), 0.5% Tween 20, and 0.5% Triton-X 100 to create a buffer solution.

2. For PFA fixed samples, block and permeabilize the sample in 200  $\mu$ L of the buffer solution for 1 h at RT.
3. Add APOE primary antibody diluted at 1:100 in the buffer solution and incubate overnight at RT.
4. The following day, wash the samples 3 times with 1x DPBS.
5. Add a secondary antibody at 1:1000 dilution in the buffer solution and add 200  $\mu$ L of the solution to the cells for 1 h at RT.
6. Wash 3 times with 1x DPBS and store samples at 4  $^{\circ}$ C, immersed in 200  $\mu$ L of DPBS.

**NOTE:** If conducting an experiment on transwells instead of a 96-well plate, samples can be mounted on a slide with mounting media (Fluoromount), covered with a glass coverslip, and sealed with transparent nail polish. Care should be taken to mount the sample with the cells facing up.

## 6. Image automation and processing

### 1. Automated image scan

**NOTE:** Zeiss LSM 800 inverted confocal scanning microscope and ZEN 3.2 (blue edition) software were used in this study. Ensure the 96-well plate is warmed to RT for a minimum of 60 min before imaging to avoid focal plane drift during the scan due to a change in the refractive index of the medium with temperature change.

1. Using a confocal microscope and a 40x objective, create a scan profile with the appropriate fluorescent channels for the lipid marker used and any additional antibodies.
2. Use the **Tiles** checkbox to set up image automation. To calibrate the 96-well plate, ensure the correct sample carrier measurements are entered and

selected. Then, click the **Calibrate** button to calibrate the plate according to the instructions, which requires using the 10x objective.

3. Choose the **Advanced Setup** view to select appropriate wells and add 3 different imaging points near the center of the well using the **Positions** function. This can be done manually under the **Position** subtab or randomly using the **Position Setup** tab and selecting **Setup by Carrier**. Repeat for all the wells of the same staining.
4. For optimal focusing and Z-stack positioning during automation, go to the **Focus Strategy** tab to select **Use Focus Surface/Z values Defined by Tiles Setup**. Alternative methods can use other focus strategies, but it is recommended to use this setting for the most consistent results.
5. Under the **Tiles** tab, click **Verify Positions** and manually set the central Z plane for each position. The settings in the **Options** subtab will order the acquisition of images, so check this before starting to image. To acquire images in the order the positions were selected, deselect the **Tile Regions/Positions** and **Carrier Wells/Container** checkboxes. Select **Split Scenes into Separate Files** for ease of image processing.
6. Ensure the **Z-Stack** tab is set to **Center**, a range is inputted to the user's preferences, and the **Optimal** button is selected to set the slice interval.
7. After optimizing the **Acquisition Mode, Channels, Focus Strategy, Z-Stack**, and **Tiles** tabs, start the experiment.

## 2. Image processing

1. Using a batch image processing method, create maximum projections of each Z-stack with the **Extended Depth of Focus** method.
2. Using a batch image processing method, export the maximum projection files as 16-bit TIFF images. Set the compression to **None** and ensure **Original Data** is checked. The resulting image should be a maximum projection greyscale TIFF of only the fluorescence channel on which the lipid marker is expressed.

## 7. Segmentation and quantification

**NOTE:** The LipidUNet program was trained on 40x images from a 96-well plate. It is highly recommended to use images that were obtained using a 40x objective.

1. Install the LipidUNet software. LipidUNet can be downloaded from the following GitHub repository: <https://github.com/RPEGoogleMap/LipidUNet>
2. Identify the TIFF images representing either Nile Red, Bodipy, or APOE and move them into a folder named **imgs** within a directory named either **Nile\_Red**, **Bodipy**, or **APOE**, depending on the method being used.
 

**NOTE:** Exact naming conventions must be used for the LipidUNet program to recognize the directories.
3. Open the LipidUNet software (**Figure 4**).
4. In the **Predict** tab of the software, select the relevant directory (**Nile\_Red**, **Bodipy**, or **APOE**) by clicking on the ellipsis and navigating to the named directory. Confirm that the LipidUNet program has correctly identified the images by checking the Class entry.
5. Select a probability threshold for the algorithm between 0.01 and 0.99. A higher value will eliminate more false

positives but might cause more false negatives, and lower values might introduce more false positives while eliminating more false negatives. A value of 0.65 is the default and is recommended.

6. Click **Predict**.

**NOTE:** The software will iterate through all the images automatically and create a new folder called `predicted_masks` in the selected directory.

7. Use a **Mask Analysis** tool to iterate through the generated masks and provide a quantitative count of the thresholded lipid deposits from the mask images.
8. Analyze the generated counts data to compare treatment conditions.

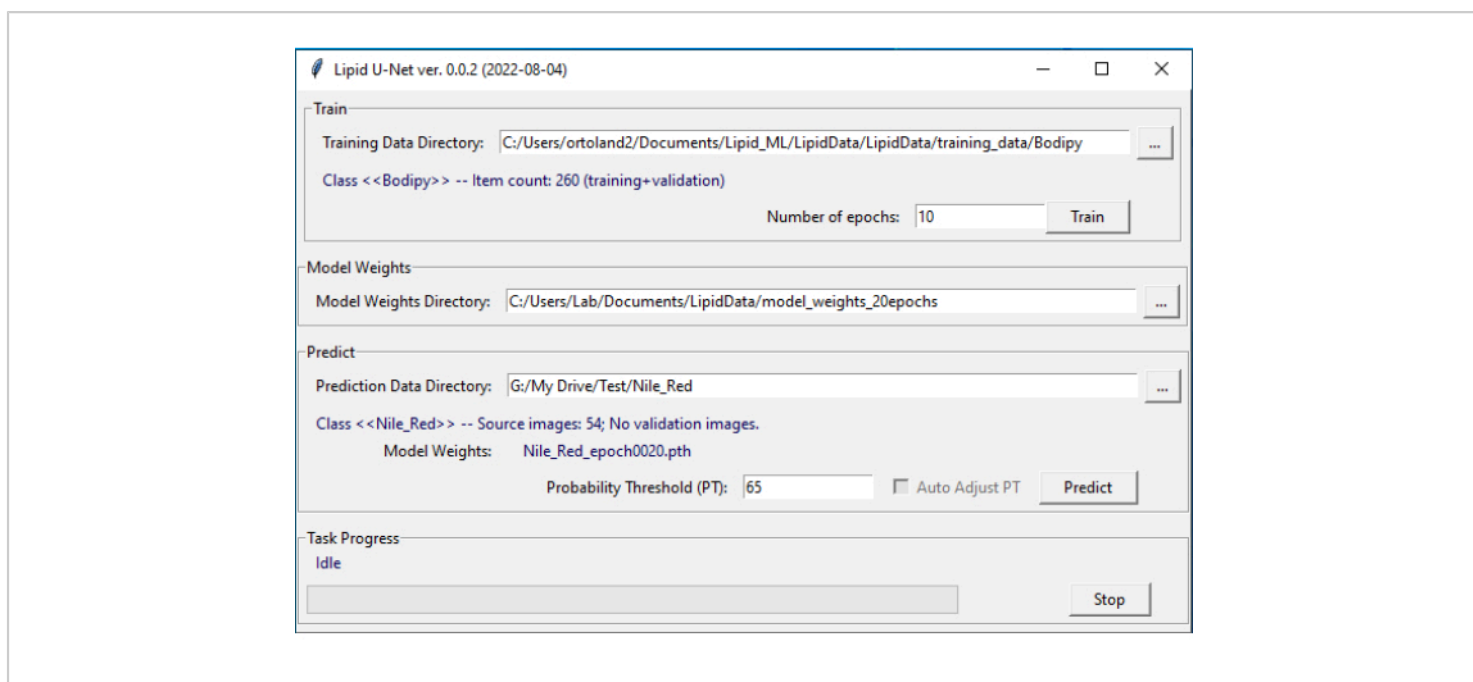


**Figure 4: LipidUNet user interface.** The LipidUNet software has different sections to select for the training data directory, where images of lipid deposits have been identified correctly; the model weights directory, which is produced from the training data; and the prediction data directory in which the user will input their images for segmentation. [Please click here to view a larger version of this figure.](#)

## Representative Results

This protocol provides a workflow to identify lipid deposits stained by Nile Red, BODIPY, and APOE. The developed software can automatically identify and quantify lipid deposits and performs best when the protocol outlined is optimized.

Included are examples of successfully differentiated RPE (**Figure 3A**) and poorly differentiated RPE (**Figure 3B**), as the quality of the cell model greatly impacts the quality of proper image segmentation.

Two of the three markers described in the protocol, Nile Red and BODIPY, are identified as small circular points

that are distinctly bright in fluorescent images (**Figure 5** and **Figure 6**). A "positive" image from the protocol would be an appropriate identification of these distinct deposits (**Figure 5A-D** and **Figure 5E-H**). A "negative" result would show incorrect segmentation of the image by mistaking background fluorescence as a deposit, either due to weak staining (**Figure 6A-C** and **Figure 6D-F**) or due to high background intensity (**Figure 6G-I**).

APOE deposits have a variety of sizes and shapes, appearing more oval or irregular rather than the circular deposits of Nile Red and BODIPY. These deposits are also less punctate, and signal intensity can differ between deposits due to variations in the permeabilization of the sample. Correct identification will identify each deposit, including those that are less saturated (**Figure 5I-L**), while incorrect segmentation will not pick up these deposits (**Figure 6J-L**). Therefore, it

is important to optimize staining and imaging methods to avoid drastic variation. One way to do this is by paying careful attention to the sample permeabilization steps while immunostaining. To optimize fluorescent signal, cells can be lysed prior to fixation and immunostaining for APOE, which results in even saturation and better segmentation of the APOE deposits.

Provided are also segmented images of cells matured on a culture platform other than a 96 well plate. The LipidUNet software was run on images of cells cultured on a transwell, and while the lipid deposits are thresholded, so too are the pores in the transwell membrane (**Figure 6M-O**). Because of the similarity in shape and size, the LipidUNet software in its current form will mask both the lipid deposits and transwell pores indiscriminately.

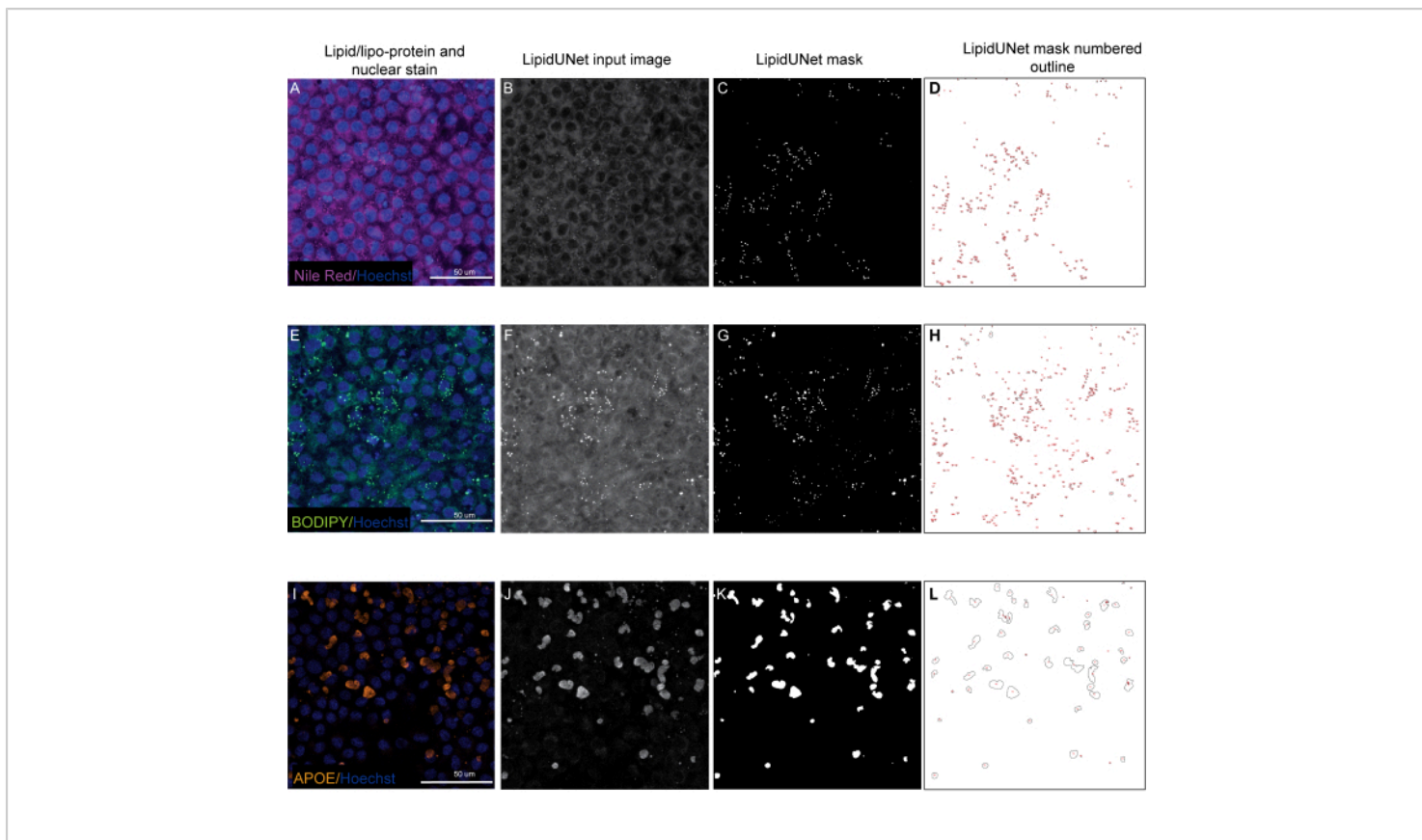


**Figure 5: Representative Results.** (A,E,I) 96-well plated RPE are stained with Hoechst nuclear staining (blue) and either Nile Red (magenta), BODIPY (green), or APOE (orange) and are the maximum intensity projections of a Z-stack. (B,F,J) The greyscale input images for the LipidUNet software after image processing. (C,G,K) Masks generated by LipidUNet, where all deposits are identified correctly. (D,H,L) Outlines of each masked particle are numbered. These labels allow to connect each particle in the image to an entry in the spreadsheet with the raw data. (A-D) shows Nile Red staining, and the software is able to recognize the deposits against the background accurately despite a weaker signal. (E-H) shows a strong contrast between the BODIPY signal and background, which is ideal. LipidUNet correctly identifies every deposit in the image. (I-L) shows a strong APOE signal and represents the variability of signal saturation that is often seen with this stain. Nonetheless, image segmentation is able to identify the borders of each APOE deposit. [Please click here to view a larger version of this figure.](#)

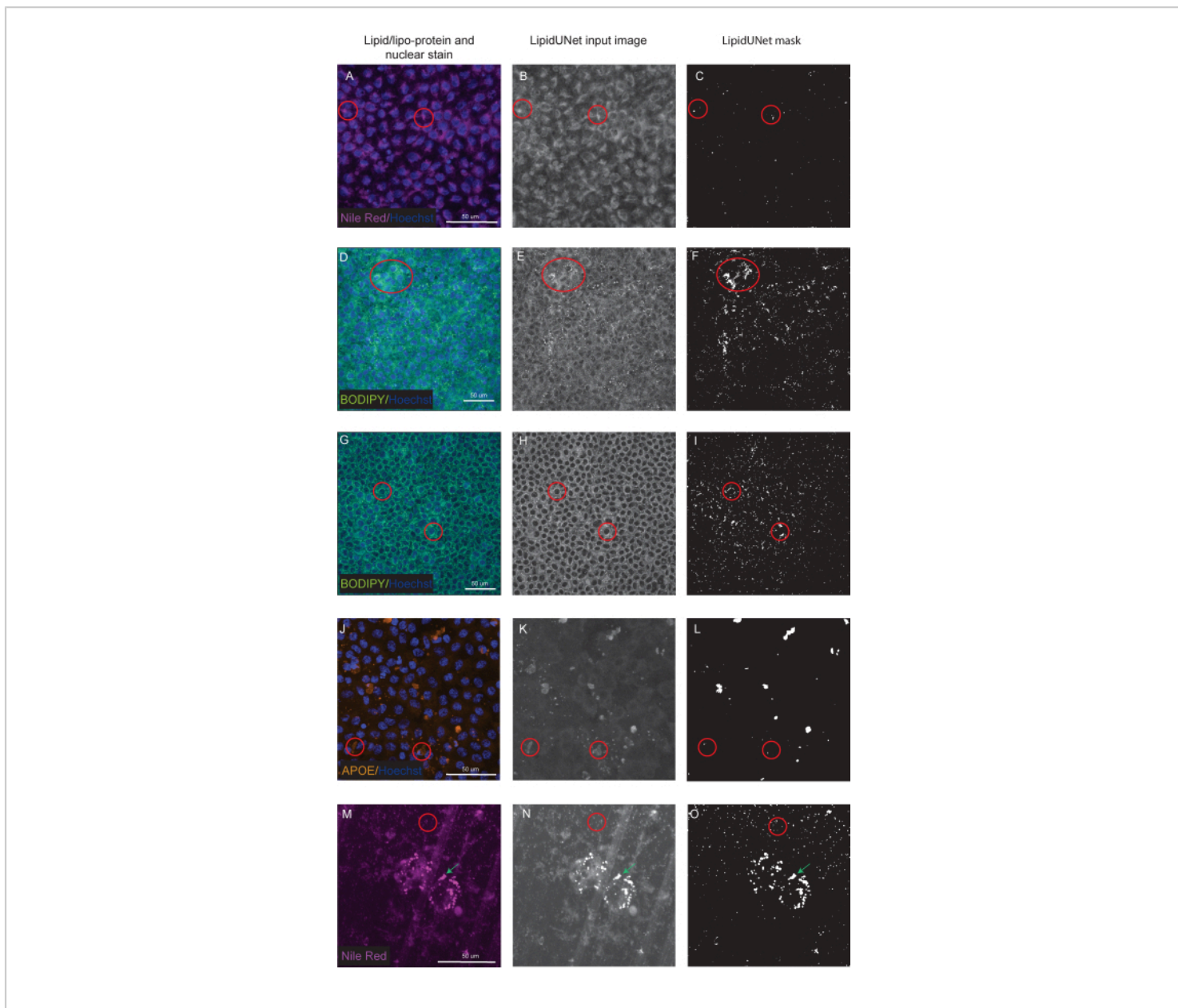


**Figure 6: Suboptimal Results.** (A,D,G,J,M) 96-well-plated RPE are stained with Hoechst nuclear staining (blue) and either Nile Red (magenta), BODIPY (green), or APOE (orange) and are the maximum intensity projections of a Z-stack. (B,E,H,K,N) The greyscale input images for the LipidUNet software after image processing. (C,F,I,L,O) The incorrect masks generated by LipidUNet. Red circles indicate where the software has incorrectly identified a lipid deposit. (A-C) Nile Red processing is incorrect because the software has identified the background staining as a deposit. This can happen more often when there is high background but few lipid deposits in the image. Two examples of BODIPY staining are shown: a poor-quality image due to (D-F) weak BODIPY staining and (G - I) a strong BODIPY signal with high background. In both cases, the software is unable to distinguish small, circular lipid deposits from the background circular ring surrounding the nucleus. While staining and imaging should be optimized to avoid these errors, the most recent version of LipidUNet is

largely improved for these images. (J-L) Incorrect APOE segmentation. Since the deposits are more variable in size and saturation of signal, the software has difficulty recognizing some deposits. (M-O) RPE seeded onto a transwell and stained with Nile Red. A slice of the Z-stack is shown here with both Nile Red lipid deposits and transwell pores. The software is unable to distinguish between the two, as shown by the red circle containing transwell pores and the green arrow pointing to Nile Red deposits. [Please click here to view a larger version of this figure.](#)

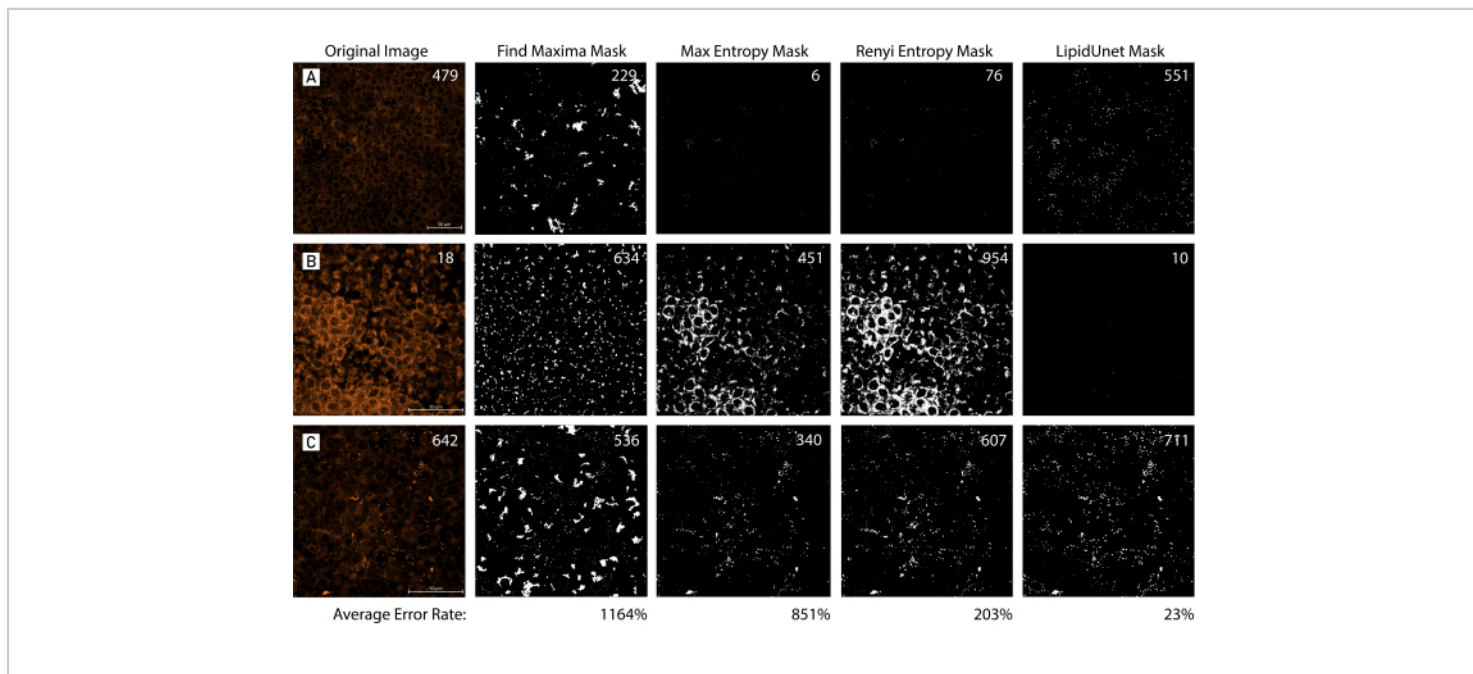


**Figure 7: Mask Tool Comparison.** (A,B,C) 96-well plated RPE with variable amounts of lipid deposition are identified with Nile Red (red). The images are masked using three different common masking methods, Find Maxima, Max Entropy, and Renyi Entropy, and compared to the LipidUNet-generated mask. The original image is accompanied by a manual count of the lipid deposits, while the masks display the predicted counts by each segmentation method. The average error rate was calculated for each method of segmentation using the following formula:  $\text{mean}[(|\text{Predicted Count} - \text{Manual Count}| / \text{Manual Count}) \times 100]$ . The LipidUNet-generated mask more accurately identifies lipid deposits across images with variable deposition when compared to other masking methods (Average error rates: 23% LipidUNet, 1164% Find Maxima, 851% Max Entropy, 203% Renyi Entropy). [Please click here to view a larger version of this figure.](#)

Component	Cat number	Stock Conc.	Final Conc.	mL
MEM alpha	12571-063	NA		500
N2 supplement	17502-048	NA	1%	5
Heat Inactivated FBS	SH30071.03	NA	5%	25
NMEM NEAA	11140-050	10mM	0.01mM	5
Sodium Pyruvate	11360-070	100mM	1mM	5
Penicillin-streptomycin	15140-122	10000u/mL	100U/mL	5
Taurine	T4571	50mg/mL	250ug/mL	2.5
Hydrocortisone	H6909	18.1mg/L	20ug/L	0.553
T3	T5516	20ug/L	0.013ug/L	0.33
Total volume, mL				548.383

**Table 1: RPE-MM reagent composition.** A list of reagents and optimal concentrations for RPE-MM.

## Discussion

This protocol provides a method to efficiently label, image, and quantify lipid deposits in monogenic and polygenic *in vitro* disease models for degenerative eye diseases. The AI-based software, LipidUNet, can be applied to three common lipid markers, APOE, Nile Red, and BODIPY, and provides a fast, automatic method for analysis that allows quantification to be standard and unbiased.

The main limitation of LipidUNet is the fact that the training dataset for the AI was limited to 40x magnification images of cells cultured in a 96-well plate. As a result of the training image set, LipidUNet, in its current form, is limited to analyzing 40x magnification images. The software can be used to analyze 40x images of cells cultured on other culture surfaces besides a 96 well plate, but care should be taken to examine the generated output masks to verify accurate thresholding by the software. More image sets (at different magnifications)

will be needed to expand the scope of what samples/images it can analyze.

The protocol has several critical steps. In the lipid marker step, the user should confirm that their chosen labeling compound (BODIPY, APOE, Nile Red) has labeled their sample effectively. Mature RPE cells are often heavily pigmented, which can impair the fluorescent signal of antibody immunostaining. When the fluorescence signal is weak or when there is too much background staining, LipidUNet cannot discern lipid droplets accurately. For a similar reason, properly selected acquisition settings for the automatic imaging step of the protocol must be used. If the images acquired are of poor quality, LipidUNet will struggle to properly mask images and therefore, quantification will be inaccurate (**Figure 6A-L**). Finally, post-processing of the images is an important step, as LipidUNet has specific requirements for the software to work.

When compared to workflows for lipid analysis that use manual thresholding, or techniques that involve automatic thresholding in software like Fiji, LipidUNet offers a nonbiased and reliable segmentation across images with variable lipid deposition, as reflected by a small error rate in the identification of lipid particles (**Figure 7**). The software allows for user entry of additional training images, allowing for analysis of image sets beyond those that utilize a 40x magnification objective or even those that utilize a different lipid marker, as outlined in the protocol. In the future, the software will be trained to analyze 3D images so that the quantification of lipid deposit volume is possible. Degenerative eye diseases that implicate lipid deposition as a major contributor to pathology are prevalent, and cases are predicted to increase as the elderly population is expanding<sup>13</sup>. Accurate disease models and efficient analysis tools, as we have outlined in this protocol, will allow for the development of novel therapeutic interventions.

## Disclosures

No disclosures.

## Acknowledgments

We thank National Eye Institute (NEI) histology core for the use of the Zeiss confocal system. This work was supported by NEI IRP funds (grant number ZIA EY000533-04).

## References

1. Kanow, M.A. et al. Biochemical adaptations of the retina and retinal pigment epithelium support a metabolic ecosystem in the vertebrate eye. *eLife*. **6**, e28899 (2017).
2. Adjianto, J. et al. The retinal pigment epithelium utilizes fatty acids for ketogenesis. *The Journal of Biological Chemistry*. **289** (30), 20570-20582 (2014).
3. Farnoodian, M. et al. Cell-autonomous lipid-handling defects in Stargardt iPSC-derived retinal pigment epithelium cells. *Stem Cell Reports*. **17** (11), 2438-2450 (2022).
4. Curcio, C. A. Soft drusen in age-related macular degeneration: Biology and targeting via the oil spill strategies. *Investigative Ophthalmology & Visual Science*. **59** (4), AMD160-AMD181 (2018).
5. Cankova, Z., Huang, J. D., Kruth, H. S., Johnson, M. Passage of low-density lipoproteins through Bruch's membrane and choroid. *Experimental Eye Research*. **93** (6), 947-955 (2011).
6. Curcio, C. A. et al. Esterified and unesterified cholesterol in drusen and basal deposits of eyes with age-related maculopathy. *Experimental Eye Research*. **81** (6), 731-741 (2005).
7. Miyagishima, K. J. et al. AMPK modulation ameliorates dominant disease phenotypes of CTRP5 variant in retinal degeneration. *Communications Biology*. **4** (1), 1360 (2021).
8. Sharma, R. et al. Epithelial phenotype restoring drugs suppress macular degeneration phenotypes in an iPSC model. *Nature Communications*. **12** (1), 7293 (2021).
9. Farnoodian, M. et al. Cell-autonomous lipid-handling defects in Stargardt iPSC-derived retinal pigment epithelium cells. *Stem Cell Reports*. **17** (11), 2438-2450 (2022).
10. Hallam, D. et al. An induced pluripotent stem cell patient specific model of complement factor H (Y402H) polymorphism displays characteristic features of age-related macular degeneration and indicates a beneficial

role for UV light exposure. *Stem Cells (Dayton, Ohio)*. **35** (11), 2305-2320 (2017).

11. Sharma, R., Bose, D., Montford, J., Ortolan, D., Bharti, K. Triphasic developmentally guided protocol to generate retinal pigment epithelium from induced pluripotent stem cells. *STAR Protocols*. **3** (3), 101582 (2022).
12. Issa, P. C., Barnard, A. R., Herrmann, P., Washington, I., MacLaren, R. E. Rescue of the Stargardt phenotype in *Abca4* knockout mice through inhibition of vitamin A dimerization. *Proceedings of the National Academy of Sciences of the United States of America*. **112** (27), 8415-8420 (2015).
13. GBD 2019 Blindness and Vision Impairment Collaborators. Causes of blindness and vision impairment in 2020 and trends over 30 years, and prevalence of avoidable blindness in relation to VISION 2020: the Right to Sight: an analysis for the Global Burden of Disease Study. *Lancet Global Health*. **9** (2), e144-e160 (2021).